CHAPTER 11

DECAY PATHWAYS OF PYRIMIDINE BASES: FROM GAS PHASE TO SOLUTION

WEI KONG*, YONGGANG HE[1], AND CHENGYIN WU[2]
Department of Chemistry, Oregon State University, Corvallis, Oregon 97331, USA

Abstract: We use a variation of the pump-probe technique to unravel the photodynamics of nucleic acid bases and their water complexes. Our work aims at bridging studies from the gas phase with those in the solution phase. Our results indicate that the intrinsic properties of the pyrimidine bases can be dramatically modified by the surrounding environment. As isolated species, the bases exhibit fast internal conversion into a long lived dark state. We present evidence and discuss the nature of this electronic state. When surrounded by water molecules, however, the bases in the dark state can be quenched effectively, and the dark state becomes unobservable to our nanosecond laser system. Although contradictive to the long held belief that DNA bases possess intrinsic photostability under UV irradiation, our conclusion offers a consistent explanation to all reported experimental and theoretical results, both prior to and after our work. The long lifetime of the dark state implies that in the early stages of life's evolution prior to the formation of the ozone layer, the abundant UV flux should have limited the existence of these bases, let alone their evolution into complex secondary structures. A protective environment, such as water, is crucial in the very survival of these carriers of the genetic code

Keywords: DNA Bases, Internal Conversion, Intersystem Crossing, Lifetime, Relaxation Mechanisms

11.1. INTRODUCTION

Recently, there has been a surge in applying gas phase spectroscopic techniques for studies of biologically relevant species [1–9]. Laser desorption with supersonic cooling has fundamentally solved the problem of vaporization of non-volatile species [5, 7]. Electrospray ionization coupled with ion trapping and cooling has

* Corresponding author, e-mail: wei.kong@oregonstate.edu
[1] Current Address: Department of Chemistry, California Institute of Technology, Pasadena, California 91125, USA
[2] Current Address: School of Physics, Beijing University, Beijing, P. R. China, 100871

M. K. Shukla, J. Leszczynski (eds.), Radiation Induced Molecular Phenomena in Nucleic Acids, 301–321.

also enabled multiply charged ions to be interrogated spectroscopically [8–10]. In the meantime, theoretical developments in ab initio and semi-empirical methods for both static and dynamic properties of large molecular systems, and sometimes even with the inclusion of the solvent environment, have also gained tremendous momentum [11–14]. It is now time for a systematic investigation of the intrinsic properties of biologically related monomers and oligomers, and for a thorough study of the role of the solvent environment in affecting the photochemical and photophysical properties of biological systems.

Experimental data of biologically related monomers in the gas phase are important in calibrating the accuracy of theoretical calculations, and in some cases, this type of information bears direct relevance to biological processes in vivo [9, 15]. Nevertheless, a wide culture gap between biochemists and gas phase physical chemists still exists. From a biochemist's point of view, isolating a monomeric species in the gas phase for a detailed interrogation bears no relevance to the complex process in a biological environment. However, for a few systems that have been studied in the gas phase [9, 15], the results are directly applicable to the fundamental biological reaction. For example, the red Opsin shifts of Schiff-base retinal chromophores in proteins were discovered to be blue shifts in reference to the isolated species [16]. This discovery calls for a new interpretation of the role of the protein environment in color tuning the visual pigments. In addition, without the data from the gas phase for calibration, any ab initio or semi-empirical calculation will have no reality check.

There are two issues that gas phase studies have to resolve when biologically related species are interrogated. On one hand, most of these species do not have well resolved rovibrational spectroscopy. Rather, they are dominated by fast internal conversion (IC) intersystem crossing (ISC). Consequently, only in a few exceptional cases are high resolution spectroscopic methods applicable. Similarly, many methods for studies of dynamical behaviors are also limited in application [17]. On the other hand, to make any gas phase observations informative in deciphering the chemistry in the solution phase, effects of the solvent have to be addressed. Occasionally, solvent/solute interactions dominate, while intrinsic properties of the isolated species become secondary. In this work, we attempt to showcase our work on dynamical studies of nucleic acid bases using a variation of the pump-probe technique, and we also demonstrate that through the formation of solute/solvent clusters, we can obtain information that is directly applicable in biological environments.

The photophysics and photochemistry of nucleic acid bases bear direct relevance to mutation of DNA under ultraviolet (UV) irradiation [18, 19]. For this reason, experimental and theoretical attempts have been made to investigate the energy transfer in nucleic acid bases, nucleosides and nucleotides [20, 20–25]. In the solution phase, the lifetime of the first bright electronically excited state S_2 has been determined to be on the order of 1 ps [22–25]. The mechanism of decay has been considered to be fast internal conversion to the ground state. The local heating effect of the absorbed photon can reach 1000 K in vibrational temperature [22]. The origin of this fast quenching effect is attributed to the extensive hydrogen bond

network in the water solution or effective energy transfer among stacked bases [26]. In the gas phase, vibronic structures of guanine, adenine and cytosine have been observed and assigned to different tautomers [5, 27–30], but two pyrimidine bases, uracil and thymine, showed structureless resonantly enhanced multiphoton ionization (REMPI) spectra [31]. In a femtosecond pump-probe experiment, Kim's group has determined the lifetime of the S_2 state to be on the same order as that in the water solution [21]. Without the solvation environment, the bases in the gas phase are deprived of relaxation partners, and the ultimate fate of the electronic energy is therefore deeply puzzling.

Our study of the photostability issue of nucleic acid bases began with isolated bases, and later extended to their water complexes [15, 32]. Our observation has thus revealed not only intrinsic properties of the bases, but also the effect of the environment on the decay mechanism of the excited state. Most of our results have been obtained from 1,3-dimethyl uracil (DMU) due to the ease of vaporization. To generalize our conclusion, however, we have also investigated 1-methyl uracil (MT), thymine (T), and 1,3-dimethyl thymine (DMT). In particular, we believe that 1-methyl uracil is an excellent mimic of uradine because of the similar substitution position on uracil.

11.2. EXPERIMENTAL METHOD

The experimental apparatus, as shown in Figure 11-1, was a standard molecular beam machine with a heated pulsed valve for vaporization of the non-volatile species and for supersonic cooling. Samples of 1-methyluracil, 1,3-dimethyluracil and thymine were purchased from Aldrich Co. and used without further purification. The sample 1,3-dimethylthymine was synthesized from thymine following a literature procedure [33], and its purity was checked by nuclear magnetic resonance (NMR) and infrared absorption (IR) spectroscopy. The heating temperatures varied for different samples: 130°C for DMU, 150°C for MU, 180°C for DMT, and 220°C for thymine. No indication of thermal decomposition was observed at these

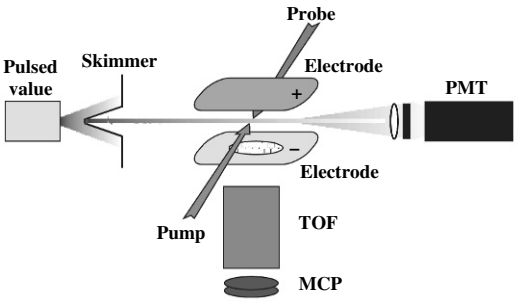

Figure 11-1. Experimental apparatus. The sample is supersonically cooled and intercepted by counter-propagating laser beams. Both fluorescence and ion signals can be observed

temperatures based on the mass spectrum obtained using non-resonant multiphoton ionization. The vapor was seeded in 2 atm of helium gas, and the gaseous mixture was expanded into a high vacuum chamber at a 10 Hz repetition rate through a 1 mm orifice. Water complexes were formed by bubbling the carrier gas through a room temperature water reservoir (vapor pressure: $\sim$ 23 mbar) before being routed to the heated sample.

A Nd:YAG (Continuum, Powerlite 7010) pumped optical parametric oscillator (OPO, Continuum, Panther) and a Nd:YAG (Spectra Physics GCR 230) pumped dye laser (LAS, LDL 2051) were used in these experiments. In the REMPI experiment, the two lasers were set to counterpropagate; and the light path, the flight tube, and the molecular beam were mutually perpendicular. The delay time between the two lasers was controlled by a delay generator (Stanford Research, DG535). Two different types of $1+1'$ REMPI experiments were performed, by either scanning the resonant or the ionization laser. In the laser induced fluorescence (LIF) experiment, the molecular beam was intercepted by the laser beam from the OPO laser; and the signal was detected by a photomultiplier tube (PMT, Thorn EMI 9125B) through two collection lenses in the direction opposite the molecular beam. In order to reject scattered light, masks were used to cover all the windows and lenses, and cut-off filters were inserted in front of the PMT. Using a Tektronix TDX350 digital oscilloscope, the time resolution of the fluorescence signal was essentially limited by the width of the laser pulse ($\sim$ 5 ns). The wavelength region of the fluorescence signal was determined using long pass filters.

11.3. RESULTS

11.3.1. Bare Molecules

Figure 11-2 shows the $1+1$ (one color, dashed line) and $1+1'$ (two color, solid line) resonantly enhanced multiphoton ionization spectra together with the gas phase UV absorption spectrum of 1,3-dimethyl uracil (dotted line). The absorption spectrum was taken at 140°C in a gas cell using a conventional UV/VIS spectrometer, while the REMPI spectra were obtained from a supersonic jet with the pulsed valve heated to the same temperature. In the one color experiment, a second order dependence of the ion signal on the laser intensity was observed, while in the two color experiment, the single photon nature of each excitation step was confirmed from a linear dependence of the ion signal on both laser beams. The delay between the pump and the probe laser in the two color experiment was 10 ns, and the probe laser was set at 220 nm. The two features in the UV absorption spectrum were assigned as the second and third excited singlet state, S_2 and S_3, and both were believed to have $\pi\pi^*$ characters [34]. The one color REMPI spectrum more or less traces the absorption curve for the S_2 feature, while the missing S_3 feature is solely a result of the low output power of the OPO laser. Limited by the non-flat tuning curve of the OPO laser, artificial structures caused by the scanning laser were observed and smoothed out. For this very reason, neither REMPI spectrum was normalized by

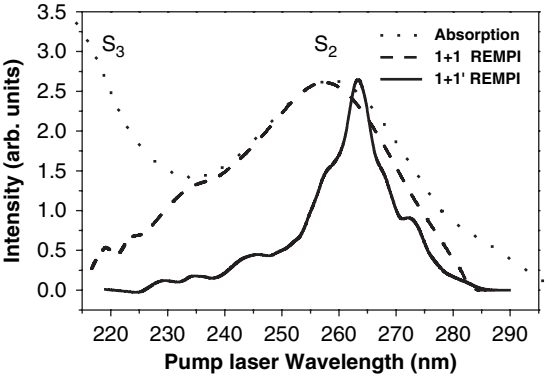

Figure 11-2. $1+1$ REMPI, $1+1'$ REMPI and UV absorption spectra of 1,3-DMU [15]. The $1+1'$ REMPI spectrum was obtained by scanning the pump laser and setting the probe laser at 220 nm with a delay time of 10 ns. Neither REMPI spectrum was normalized by the laser power, and at the short wavelength side of the figure, the low output power of the OPO laser resulted in the missing S_3 feature in the $1+1$ spectrum. The absorption spectrum was taken at 140°C, the same temperature as that of the pulsed valve during the REMPI experiments. (Reproduced with permission from J. Phys. Chem. 2004, 108, 943–949. Copyright 2004 American Chemical Society.)

the intensity of the OPO laser. When divided by the square of the laser power, the one color REMPI spectrum indeed peaked up again in the vicinity of the S_3 feature. In Figure 11-2, the one color REMPI spectrum shows slightly higher energy onset than that of the absorption spectrum, possibly due to supersonic cooling in the REMPI experiment. The $1+1'$ REMPI spectrum, on the other hand, shows clear differences from the one color spectrum. It has a much narrower feature between 285 nm and 240 nm, and its center is slightly shifted to a lower energy. Under the same experimental conditions, no two color signal was obtained when the resonant laser scanned further into the S_3 region, even after taking into account the low output power of the OPO laser.

The solid line in Figure 11-3 shows the result of a different REMPI experiment, while the dashed line is from the one laser experiment discussed in Figure 11-2. Immediately after finishing the one color $1+1$ REMPI spectrum (dashed curve) by scanning the OPO laser, we introduced a dye laser beam at 250 nm 10 ns before the OPO laser, and rescanned the same wavelength region using the same OPO laser at the same laser energy. The intensity of the dye laser was carefully controlled so that it generated no ion signal by itself, and when the OPO scanned through the region between 240 and 217 nm, a first order dependence of the two laser ion signal on the power of the dye laser was obtained. This experiment is notably different from a typical $1+1'$ REMPI experiment, and it is referred to as a "two laser" experiment in the following. Similar to Figure 11-2, neither spectrum in Figure 11-3 was normalized by the power of the OPO laser, and the precise shapes of the observed features are unimportant to the present discussion. The two laser spectrum in Figure 11-3 shows a sharp rise at the short wavelength region despite of the drop in the power of the OPO laser. Qualitatively, a thirty-fold increase in the ion

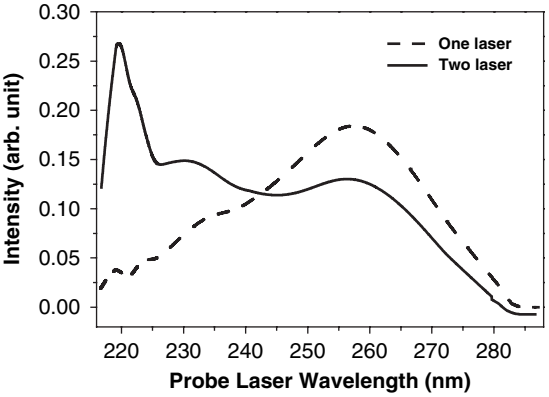

Figure 11-3. Effect of the pump laser at 250 nm with a time advance of 10 ns on the one laser REMPI spectrum of the probe laser [15]. Both spectra were recorded using the same intensity for the probe laser. The pump laser in the two laser experiment resulted in a maximum depletion of 20–25% in the region between 245 and 280 nm, and an enhancement of three decades at 220 nm. See text for a detailed explanation of the experimental method. (Reproduced with permission from J. Phys. Chem. 2004, 108, 943–949. Copyright 2004 American Chemical Society.)

signal at 220 nm is observable. In contrast, when the OPO laser is at a wavelength between 245 and 280 nm, the early arrival of the pump laser causes a depletion of ~25% of the one color ion signal. This depletion/enhancement effect was also observed to be sensitive to the delay between the two lasers, but insensitive to the pump wavelength of the dye laser within the absorption profile of the S_2 state.

Figure 11-4 shows a pump-probe transient of 1,3-DMU with both laser beams in the S_2 region: the pump beam at 265 nm, while the probe beam at 248 nm. The profile is fitted by a Gaussian function with a time constant (full width at

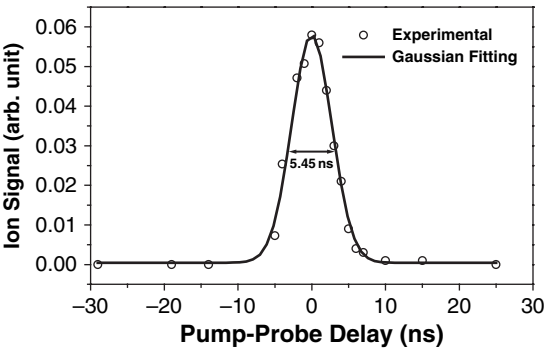

Figure 11-4. Pump-probe transient ionization signal of 1,3-DMU in the gas phase with the pump and probe wavelengths at 265 and 248 nm, respectively [15]. The time constant (full width at half maximum) for the Gaussian function is 5.45 ns. (Reproduced with permission from J. Phys. Chem. 2004, 108, 943–949. Copyright 2004 American Chemical Society.)

half maximum) of 5.54 ns. Kang et al. reported the lifetimes of the S_2 state of the pyrimidine bases to be in the range of several picoseconds using their femtosecond laser system [21]. Thus Figure 11-4 confirms that the lifetime of the S_2 state is indeed much shorter than our instrumental response, and that our time resolution is on the order of 5.5 ns.

In contrast, Figure 11-5 shows the pump-probe transient of 1,3-DMU with the probe wavelength at 220 nm, while the pump wavelength was maintained within the S_2 region at 251 nm. On the scale of the figure, the ion signal due to either one laser alone was insignificant, and the overall signal intensity showed linear dependence on the power of both lasers. The solid line in the Figure represents a fitting result by assuming a convolution of a single exponential decay function and a Gaussian function (dashed line). The time constant of the Gaussian function agrees with that of Figure 11-4. In Figure 11-5, the signal reaches its maximum at a delay time of 8 ns between the two beams, and then it decays to the background level exponentially. This time response is clearly different from the picosecond decay reported by Kang et al. [21], and the involvement of another totally different state, i.e., a dark state, has to be invoked.

The lifetime of this dark state demonstrates explicit dependence on the wavelength of the pump beam and the degree of substitution on the uracil ring. Figure 11-6 summarizes the results on the four pyrimidine bases investigated in this work. The general trend is that the more substituted the ring and the longer the pump wavelength, the longer the lifetime of the dark state. Moreover, substitution at the –1 position is more effective than at the –5 position in stabilizing the dark state.

To further assess the fate of the molecules in the excited state, we attempted to observe the fluorescence signal, but the signal was so weak that a quantitative measurement of the dispersed spectrum was impossible using our existing setup. However, by recording the decay profile, the fluorescence lifetimes were obtained

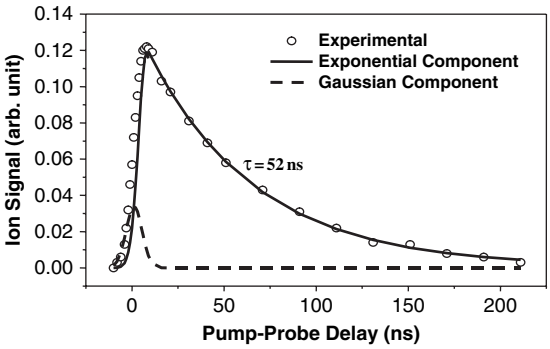

Figure 11-5. Pump-probe transient ionization signal of 1,3-DMU in the gas phase with the pump and probe wavelengths at 251 and 220 nm, respectively. Hollow circles represent experimental data, and the solid line is a theoretical fit including a single exponential decay convoluted with the instrumental response (*dashed trace*). The exponential decay constant is 52 ns, while the full width at half maximum of the Gaussian function is 5.5 ns

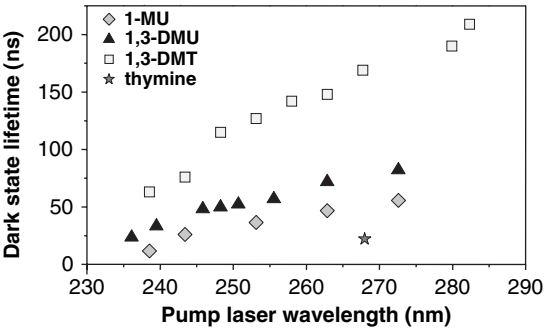

Figure 11-6. Lifetimes of 1-methyl uracil, 1,3-dimethyl uracil, 1,3-dimethyl thymine, and thymine at different excitation wavelengths. (Reproduced with permission from J. Phys. Chem. 2004, 108, 943–949. Copyright 2004 American Chemical Society.)

at different pump wavelengths. Figure 11-7 shows two typical fluorescence decay curves. The oscillations in these profiles were caused by an electrical problem of our detection system. All decays could be fitted to single-exponential functions, with constants ranging from 18 ns at 236 nm to 54 ns at 260 nm for 1,3-DMU. These values were obtained without corrections of the instrumental response, so they should be regarded as qualitative rather than quantitative. Nevertheless, these fluorescence lifetimes are in good agreement with the decay time of the REMPI signal in Figure 11-6. Using long pass filters, we determined that the peak of the radiation was centered between 370 and 440 nm.

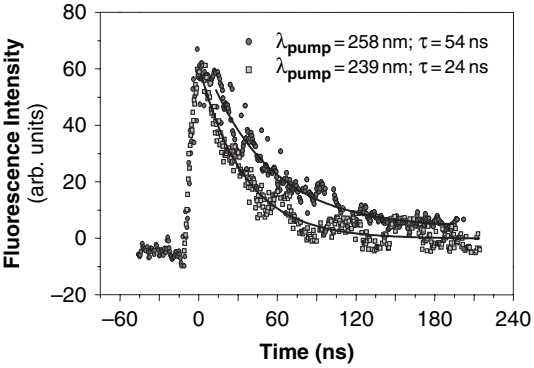

Figure 11-7. Fluorescence signal of 1,3-DMU in the gas phase at different excitation wavelengths [15]. Solid curves are best fits to the experimental data. The oscillations in the decay curves were caused by an electrical problem in our detection system. (Reproduced with permission from J. Phys. Chem. 2004, 108, 943–949. Copyright 2004 American Chemical Society.)

11.3.2. Hydrated Clusters

The relevance of the dark state to a biological system in water can be elucidated from studies of hydrated complexes. Through the sequential addition of water molecules to thymine, we can observe the gradual change in photophysics as we build up the solvent environment.

Figure 11-8 compares the transients of thymine and $T(H_2O)_1$ obtained from a two color $1+1'$ experiment. With the pump wavelength at 267 nm and the ionization wavelength at 220 nm, the lifetimes of the dark state of thymine and $T(H_2O)_1$ were measured to be 22 ns and 12 ns respectively. The fact that the decay profile of $T(H_2O)_1$ contains only a single exponential decay function is evidence that this measurement was not contaminated by dissociative products of larger complexes. For clusters containing two or three water molecules, the two color signal was too weak for an accurate determination of the decay constant. However, as we increased the delay time between the pump and the probe laser, we observed that heavier clusters disappeared faster than lighter ones. We therefore conclude that this decrease in lifetime with increasing water content is gradual in complexes with $n < 5$. No two color ion signals were observable for clusters with four or more water molecules.

Another interesting observation in this study is the dependence of the mass spectrum on the excitation energy in the one laser $1+1$ experiment. We observed that from 220 nm to 240 nm (the absorption region of the S_3 state of the bare molecule), small water clusters with n up to 4 were readily observable, as shown in Figure 11-9a, while in the region of 240 to 290 nm (the absorption region of the S_2 state of the bare molecule), these hydrated cluster ions were conspicuously missing or barely detectable in Figure 11-9b. This wavelength dependence is summarized in Figure 11-10, where the intensity of each cluster ion is normalized at 220 nm to highlight the dynamics at the S_2 state. At 220 nm, all cluster ions with $n \leq 5$ can be clearly seen, suggesting the existence of the corresponding neutral clusters

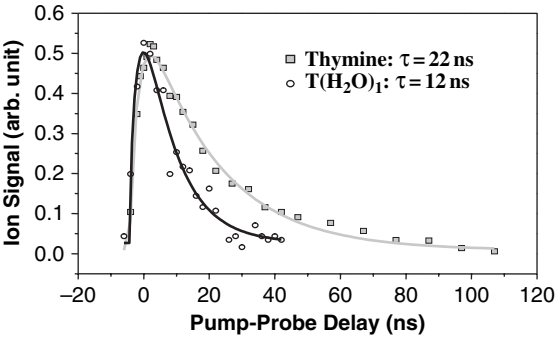

Figure 11-8. Pump-probe transients of bare thymine and $T(H_2O)_1$ in the gas phase with the pump and probe wavelengths at 267 and 220 nm, respectively. (Reproduced with permission from J. Phys. Chem. 2004, 108, 943–949. Copyright 2004 American Chemical Society.)

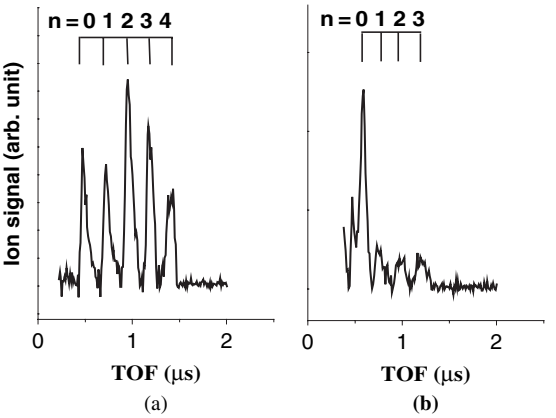

Figure 11-9. One-color REMPI mass spectra of hydrated thymine clusters, obtained at the excitation wavelengths of 229 nm (a) and 268 nm (b) respectively. (Reproduced with permission from J. Phys. Chem. 2004, 108, 943–949. Copyright 2004 American Chemical Society.)

in our source. In the absorption region of the S_2 state, however, the attachment of one water molecule decreases the ion signal to half of its value compared with that of the bare molecule. Additional attachment of one or two water molecules has a similar effect. When four or more water molecules are attached, the S_1 state is no longer observable from the ionization spectrum. Since the ionization energy (IE) of thymine is 9.15 eV, corresponding to 271 nm in this one laser experiment, and $T(H_2O)_n$ clusters are believed to have even lower IEs [35], the lack of heavy ions in the S_2 region cannot be attributed to the low excitation energy. This loss of heavy

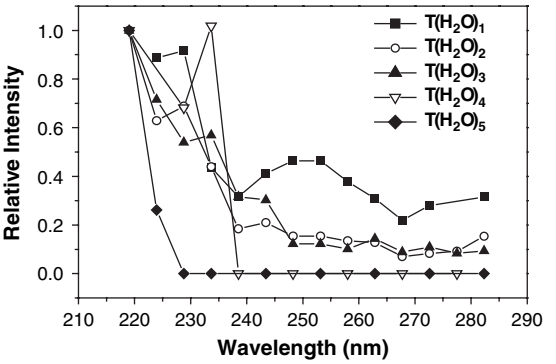

Figure 11-10. Intensity variations of cluster ions at different excitation wavelengths in a one laser 1 + 1 REMPI experiment. The intensities of different sized cluster ions were normalized at 220 nm (S_3 state) to highlight the dynamics at the S_2 state. (Reproduced with permission from J. Phys. Chem. 2004, 108, 943–949. Copyright 2004 American Chemical Society.)

ions in the S_2 region should therefore imply a loss of population during excitation or ionization.

11.4. DISCUSSION

11.4.1. A Dark Electronic State

The above results provide concrete evidence that the decay mechanism of methyl substituted uracil and thymine bases involves more than two states and depends on the environment. Figure 11-11 shows the proposed energy levels and processes for the pyrimidine bases in the gas phase. After initial excitation to the S_2 state, we believe that a significant fraction of the gas phase molecules decays to a dark state S_1. While the lifetime of the S_2 state is shorter than our instrumental response, the lifetime of the dark state is in the range of tens to hundreds of nanoseconds, depending on the degree of methylation and the amount of excess energy. The nature of this dark state is most likely a low lying $^1n\pi^*$ state, and further ionization from this dark state requires a much higher excitation energy. Although we are unable to provide a precise estimate of the quantum yield for this decay channel, based on our previous estimate, the lower limit should be 20% in bare molecules. Water molecules, on the other hand, can significantly reduce the lifetime of the S_2 state and enhance the IC from the dark state to the ground state. As a result, in aqueous solutions, the dark state becomes undetectable using our nanosecond laser system.

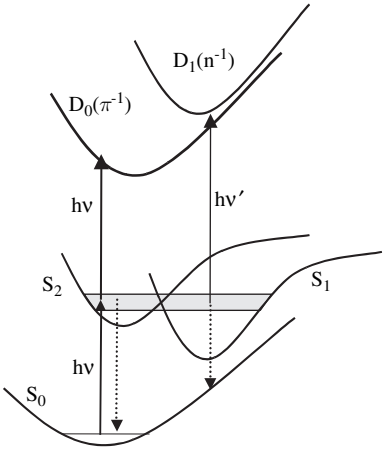

Figure 11-11. Proposed potential energy surfaces and processes for the pyrimidine bases. Ionization from the S_2 state and the dark state S_1 samples a different Franck-Condon region of the ionic state ($D_0(\pi^{-1})$) or reaches a different ionic state ($D_1(n^{-1})$), resulting in different ionization energies for these two states

This model can provide a consistent explanation of our experimental observation. The $1+1'$ REMPI signal in Figure 11-2 (solid line) is from ionization of this dark state, while the one color signal (dashed line) is from ionization of the initially populated S_2 state. The narrower width of the $1+1'$ spectrum compared with that of the one color spectrum reflects the limited energy range for effective overlap between the dark state and the S_2 state. This dark state does not absorb in the region of 245–280 nm, rather, it absorbs in a much higher energy region from 217 to 245 nm. Relaxation of the molecular frame in the dark state could result in a different Franck-Condon region for vertical ionization, or more likely, an entirely different cationic state accessible only from the dark state. In the REMPI experiment of Figure 11-3, the dye laser at 250 nm pumps a significant fraction of the overall population to the dark state. After a delay of 10 ns, the scanning OPO probes a reduced population, resulting in a loss of the overall ion signal between 245 and 280 nm. However, when the OPO scans into the absorption region of this dark state between 217 and 245 nm, all molecules either in the ground state or the dark state can be ionized. The ionization yield of the dark state is higher than that of the S_2 state in this wavelength region, hence an enhanced ion signal is observable. The decay profile in Figure 11-5 corresponds to the decay of this dark state. Fluorescence from this dark state should take place in a red-shifted region, i.e., 370–440 nm from this study, compared with that of the S_2 state (300 nm) [36]. The similarity of the decay constants of the fluorescence (Figure 11-7) and the $1+1'$ REMPI signal (Figure 11-6) confirms that in both experiments, we are probing the same dark state. Methyl substitution stabilizes this dark state as shown in Figure 11-6, while vibrational excitation destabilizes this state by opening more decay channels.

We believe that the dark state is an independent electronic state, rather than a stack of highly vibrationally excited states in the ground electronic state populated from fast internal conversion and intramolecular vibrational redistribution (IVR) [37]. This belief is based on the decay time and the signal intensity in the two laser experiment of Figure 11-3. The decay of the "recovered" molecules when the probe beam is between 217 and 245 nm is on a time scale of tens to hundreds of nanoseconds. These constants are much smaller than those from decay of hot vibrational levels after IVR under collision free conditions [37]. More importantly, the result of IVR is typically a wide spread of population in many different vibrational levels and modes, and the resulting population in each vibrational level is low. Under the excitation of a laser with a band width of less than a few wavenumbers, the ionization signal is expected to be small. The chance to observe a 30 fold increase in absorption probability is thus minimal. The concentrated population at a certain rovibronic level further implies that the dark electronic state is energetically close to the initially accessed S_2 state, and only a small degree of IVR is possible. The large Stokes shift in the fluorescence spectrum between S_2 (370 – 440 nm) and S_1 (300 nm), on the other hand, could be a mere indication of large differences in molecular geometry between S_1 and S_0.

11.4.2. Nature of the Dark State

Among the many possible candidates of the dark state, including $^1n\pi^*$, $^1\sigma\pi^*$, and $^3\pi\pi^*$, we consider a $^1n\pi^*$ state most likely, although we do not have enough evidence to exclude the possibility of a triplet state. The presence of several heteroatoms with lone pair electrons results in the existence of a number of low-lying $^1n\pi^*$ states close to the $^1\pi\pi^*$ state. These states are readily coupled to the $^1\pi\pi^*$ state by out-of-plane vibrational modes via conical intersections (CI). This type of fast state switch has been invoked to explain the extremely low quantum yield of fluorescence from the $^1\pi\pi^*$ state. Based on our assessment of the low fluorescence quantum yield of this $^1n\pi^*$ state, however, we further propose that there exists a weak conical intersection between this $^1n\pi^*$ state and the ground state, and there also is an energy barrier on the $^1n\pi^*$ surface that hinders effective population relaxation. The fact that the lifetime of the dark state drops continuously with increasing pump photon energy offers supportive evidence for the energy barrier. A recent calculation by Sobolewski et al. has shown that conical intersections between the $^1\pi\pi^*$ state and nearby $^1\sigma\pi^*$ states in aromatic biomolecular systems are ubiquitous [38]. However, the authors have stressed that this intersection relies on the polarizability of the NH or OH bond. It is therefore unclear to us whether the same mechanism would be applicable to N-methyl substituted compounds. The multiplicity of the dark state is certainly a point of debate, and our limited information is from the literature report on millisecond to second lifetimes of the triplet state for these bases in the condensed phase [39–41]. Moreover, our work on water complexes of thymine demonstrates strong quenching effect on the lifetime of the dark state with the addition of just one or two water molecules. Such a strong effect is not quite likely if the involved state is triplet in nature. Although a triplet state for the corresponding nucleosides in solutions is known to be within the same energy region as this dark state [42], a few theoretical calculations also reported simultaneous existence of singlet states [43–45].

The $^1n\pi^*$ nature is also consistent with the observed absorption and emission characteristics of the dark state. Ionization from a non-bonding orbital should yield an ionic state $D_1(n^{-1})$, and the required ionization energy is about 0.5 eV higher than that of $D_0(\pi^{-1})$ for uracil [46]. This increase in IE could be the reason for the inability to absorb between 245 and 280 nm from the dark state of DMU. If the large Stokes shift in the emission spectrum is truly representative of a large difference in equilibrium geometry between S_1 and S_0, direct absorption from S_0 would be in a much higher energy region than the adiabatic energy difference. The possibility of direct absorption from S_0 to S_1 would thus be difficult, if possible at all.

The involvement of a dark state in the decay of electronically excited states is not limited to methylated uracil and thymine. In fact, all five nucleic acid bases have demonstrated similar behaviors upon electronic excitation [27, 30]. The possibility of a low lying state that couples with the S_2 state has been suggested by Levy and co-workers to explain the broad structureless spectra of uracil and thymine in jet-cooled gas phase experiments [31]. de Vries' group has recorded vibrationally resolved

REMPI spectrum of cytosine [27], and the lifetime of the dark state is on the order of 300 ns. Mons group has studied the spectroscopy of guanine [30], and evidence for the dark state has also been reported. For adenine, the photophysical model involving two interacting electronic states has been evoked by both Kim's and de Vries' groups [47, 48]. Using picosecond time resolved $1 + 1'$ photoionization, the lifetime of the first electronically excited state of adenine has been determined by Lührs et al. [49]. The authors have also cast doubt on the generally believed model that involves direct IC to the ground state after photoexcitation. The possibility of either a low lying $n\pi^*$ state through IC or a triplet state via intersystem crossing has been suggested. The existence of a dark state in the decay pathway of nucleic acid bases has also been proposed in several theoretical studies [38, 50]. Broo has suggested that in adenine, a strong mixing between the lowest $n\pi^*$ and $\pi\pi^*$ states via the out-of-plane vibrational modes could lead to increased overlap with the vibrational states of the ground state [50]. This "proximity effect", as suggested by Lim [51], has been used in the past to explain the ultra short lifetimes of the DNA bases. To some extend, the universality of the dark state among nucleic acid bases is not too surprising, since all heterocyclic compounds are rich in unpaired electrons. Excitation of lone pair electrons is generally forbidden, which explains the dark nature of these states. On the other hand, out of plane deformation of the planar structure can easily induce interactions between these states and the optically bright π^* orbital [52].

11.4.3. Hydration and the Dark State

The effect of hydration on the decay pathway can reconcile the differences between results from the gas phase and those from the liquid phase. In the work of Wanna et al. on pyrazine and pyrimidine, a similar loss of ion signal from hydrated clusters was observed [53], and an increased rate of internal conversion upon solvation was proposed. In the case of the pyrimidine bases, however, we could not distinguish the destination of the increased IC either being the dark state or the ground state, although indications from our experimental data, including the faster decay of the dark state upon hydration, favor the dark state as the destination. Typically in a $n\pi^*$ transition, solvation by a proton donor such as water causes a blue shift; while in a $\pi\pi^*$ transition, this effect is a slight red shift [54]. The energy gap between the initially accessed $\pi\pi^*$ (S_2) and the $n\pi^*$ dark state can thus be reduced in the presence of water, and subsequently a better vibronic coupling between the two states can occur. On the other hand, we cannot exclude the possibility that IC directly to the ground state might still be somewhat competitive with IC to the dark state even in the gas phase. In the presence of water, the balance between the two decay pathways could shift, and a faster direct IC process to the ground state could also accelerate the relaxation process. In either explanation, the photophysics of the pyrimidine bases is significantly affected by the water solvent. The origin of the photostability of the pyrimidine bases therefore lies in the environment, not in the intrinsic property of these bases.

As to the change in the mass spectrum with the excitation energy in our one laser REMPI experiment in Figure 11-9, we believe it is due to the shortened lifetime of the S_2 state under water complexation. In our experiment using a nanosecond laser system, the failure to accumulate a population at the S_2 state for further ionization can only be attributed to fast depopulation from the initially prepared state, through internal conversion, intersystem crossing, or dissociation. Kim and co-workers studied hydrated adenine clusters in the gas phase [55, 56]. Using a nanosecond laser, they observed a near complete loss of hydrated adenine ions in the S_1 region, while using a femtosecond laser, all hydrated clusters were observable. They also measured the lifetime of the S_1 state to be 230 fs for $A(H_2O)_1$ and 210 fs for $A(H_2O)_2$, while the lifetime of the S_1 state of bare adenine was 1 ps. This five fold change in lifetime was apparently sufficient to cause a qualitatively different behavior under femtosecond or nanosecond excitation.

Lifetime reduction of both the dark state and the S_2 state upon hydration should be no surprise based on studies in the gas phase and in the liquid phase. For thymine, the lifetime of the S_2 state was reported to be 6.4 ps in the gas phase [21] and 1.2 ps in the liquid phase [25]. Similarly, for the other two pyrimidine bases, uracil and cytosine, the lifetimes of the S_2 states were measured to be 2.4 ps and 3.2 ps respectively in the gas phase [21], while these values decreased to 0.9 ps and 1.1 ps in the liquid phase [25]. In this work, we report a gradual decrease in lifetime with the increase of hydration. When four or more water molecules are in the vicinity, we suspect that the behavior of thymine is essentially the same as that in the liquid phase, i.e., on the picosecond time scale.

11.4.4. Further Evidence of the Dark State

Since the publication of our work, a few other experimental work using different techniques, in both gas and solution phases, and several theoretical reports, have all confirmed the existence of this long lived dark state [20, 57]. Most notable is a recent work by Kohler's group in the solution phase [58, 59]. Using the femtosecond transient absorption technique, Hare et al. [58, 59] have reported that upon photoexcitation, the pyrimidine bases bifurcate into two decay channels, and approximately 10–50% of the population decays via the $^1n\pi^*$ state with lifetimes on the order of 10–150 ps. This is a significant amendment to the original picture proposed by the same group where only fast IC from S_2 directly to S_0 was emphasized [60]. Moreover, several folds of longer lifetimes for the nucleotides and nucleosides have also been observed, revealing an unprecedented effect of the ribose group. In the gas phase, Stolow's group and Kim's group have observed long tails in their femtosecond pump-probe experiments [20, 21], and the decay time of this component is beyond the time limit of their instruments. However, Ullrich et al. have assigned a much faster component with a lifetime of 490 fs to the $^1n\pi^*$ state [20], while the authors have offered no explanation to the slow component. A discrepancy therefore emerges with regard to the lifetime of the $^1n\pi^*$ state: if it is less than half a picosecond in the gas phase, then it should not be longer

than 10 picoseconds in solution [58, 59]. Assigning the dark state and the state in solution with a lifetime of 10 ps to a triplet state would resolve this issue, but it will contradict with the reported lifetime of triplet states of several milliseconds in the condensed phase [39–41]. More experimental work, in particular, quenching experiments with triplet scavengers, is needed to clarify the situation. The existence of a singlet state in the vicinity of the dark state has also been confirmed from two independent theoretical calculations [57] (T. Martinez, 2005, Private communication). Even the lifetime of the singlet state has been modeled to be on the order of tens of nanoseconds. Moreover, in a photoinduced DNA-protein cross-linking experiment [61], Russmann et al. have observed that by delaying the pump and probe lasers with a time lag of 300 fs, the yield of cross-linking can be further enhanced. The time scale of this intermediate state is too fast in comparison with the report from Kohler's group [58, 59], but it is on the same order as that of Stolow's group [20]. The jury is still out whether this state bears any relation to the $^1n\pi^*$ state.

11.5. ORIGIN OF PHOTOSTABILITY OF NUCLEIC ACID BASES

The discovery of the dark state forces us to reconsider the origin of the photostability of nucleic acid bases. The conventional belief that natural evolution has selected these four bases as carriers of the genetic code because of their intrinsic photostability, is proven untrue. In fact, isolated pyrimidine bases can be stuck in an energetic state after absorbing a UV photon, and with so much energy stored, encounters with other species could well lead to a whole gamut of chemical reactions, from formation of radicals to loss of electrons. In particular, the high yield of ionization at 220 nm as shown in Figure 11-3 implies that there should be no neutral base exists under high UV flux conditions. Thus prior to the formation of the protective ozone layer in the upper atmosphere, the nuclear acid bases can simply not survive, let alone accumulate in concentration and ultimately evolve into an oligomeric form. In the presence of water, however, the situation becomes much more promising. With the shortening in lifetime of the dark state, the species is offered a facile deactivation pathway, and the survival probability is increased dramatically. Moreover, with further increase in concentration and ultimately with the evolution of secondary structures, base pairing and base stacking offer more protection. de Vries' group has reported that the Watson-Crick base pair is the shortest lived in the excited state among the many possible arrangements of the dimmer [5]. It is therefore reasonable to speculate that ultimately, the photochemical stability of the overall system, including the bases and their immediate environment, survives the harsh condition and dominates the primordial soup.

The photochemical stability of the nucleic acid bases under UV irradiation is no longer a major concern after the formation of the ozone layer, and the role of the $^1n\pi^*$ state in the form of modern life is significantly reduced. However, Kohler's group suspects that the $^1n\pi$ state might still be involved in the formation of photohydrates and pyrimidine/pyrimidine photoproducts, while the formation of

cyclobutane dimers is now believed to be directly through the $\pi\pi^*$ state without any potential barrier [62].

11.6. CONCLUSIONS

We present experimental results on photophysical deactivation pathways of uracil and thymine bases in the gas phase and in solvent/solute complexes. After photoexcitation to the S_2 state, a bare molecule is funneled into and trapped in a dark state with a lifetime of tens to hundreds of nanoseconds. The nature of this dark state is most likely a low lying $^1n\pi^*$ state. Solvent molecules affect the decay pathways by increasing IC from the S_2 to the dark state and then further to the ground state, or directly from S_2 to S_0. The lifetimes of the S_2 state and the dark state are both decreased with the addition of only one or two water molecules. When more than four water molecules are attached, the photophysics of these hydrated clusters rapidly approaches that in the condensed phase. This model is now confirmed from other gas phase and liquid phase experiments, as well as from theoretical calculations. This result offers a new interpretation on the origin of the photostability of nucleic acid bases. Although we believe photochemical stability is a major natural selective force, the reason that the nucleic acid bases have been chosen is not because of their intrinsic stability. Rather, it is the stability of the overall system, with a significant contribution from the environment, that has allowed the carriers of the genetic code to survive, accumulate, and eventually evolve into life's complicated form.

Our work on hydrated clusters manifests the value of gas phase experiments. Condensed phase studies reveal the properties of the bulk system. However, it is difficult to distinguish intrinsic vs. collective properties of a system. Gas phase studies, on the other hand, directly provide information on bare molecules. Moreover, the investigation of size selected water complexes can mimic the transition from an isolated molecule to the bulk. The comparison of gas phase experimental results with theoretical calculations can also provide a direct test of theoretical models. This test is in urgent need if theoretical modeling is to evolve into calculations of solvated systems with credibility.

ABBREVIATIONS

LIF	laser induced fluorescence
REMPI	resonantly enhanced multiphoton ionization
DMU	1,3-dimethyl uracil
T	thymine
IC	internal conversion
OPO	optical parametric oscillator
ISC	intersystem crossing
IVR	intramolecular vibrational redistribution

REFERENCES

1. Hunig I, Painter AJ, Jockusch RA, Carcabal P, Marzluff EM, Snoek LC, Gamblin DP, Davis BG, Simons JP (2005) Adding water to sugar: A spectroscopic and computational study of alpha- and beta-phenylxyloside in the gas phase. Physical Chemistry Chemical Physics 7:2474–2480.
2. Pratt DW (2002) Molecular dynamics: Biomolecules see the light. Science 296:2347–2348.
3. Dian BC, Clarkson JR, Zwier TS (2004) Direct measurement of energy thresholds to conformational isomerization in tryptamine. Science 303:1169–1173.
4. Gerlach A, Unterberg C, Fricke H, Gerhards M (2005) Structures of Ac-Trp-OMe and its dimer (Ac-Trp-OMe)(2) in the gas phase: influence of a polar group in the side-chain. Molecular Physics 103:1521–1529.
5. bo-Riziq A, Grace L, Nir E, Kabelac M, Hobza P, de Vries MS (2005) Photochemical selectivity in guanine-cytosine base-pair structures. Proceedings of the National Academy of Sciences of the United States of America 102:20–23.
6. Hudgins RR, Mao Y, Ratner MA, Jarrold MF (1999) Conformations of Gly(n)H(+) and Ala(n)H(+) peptides in the gas phase. Biophysical Journal 76:1591–1597.
7. Canuel C, Mons M, Piuzzi F, Tardivel B, Dimicoli I, Elhanine M (2005) Excited states dynamics of DNA and RNA bases: Characterization of a stepwise deactivation pathway in the gas phase. Journal of Chemical Physics 122:074316-1-074316/6.
8. Danell AS, Danell RM, Parks JH (2005) Dynamics of gas phase oligonucleotides. Clusters and Nano-Assemblies: Physical and Biological Systems, [International Symposium], Richmond, VA, United States, Nov.10-13, 2004393-406.
9. Nielsen IB, Lammich L, Andersen LH (2006) S1 and S2 excited states of gas-phase schiff-base retinal chromophores. Physical Review Letters 96:018304/1–018304/4.
10. Wang XB, Woo HK, Wang LS, Minofar B, Jungwirth P (2006) Determination of the electron affinity of the acetyloxyl radical (CH3COO) by low-temperature anion photoelectron spectroscopy and ab initio calculations. Journal of Physical Chemistry A 110:5047–5050.
11. Meyer EA, Castellano RK, Diederich F (2003) Interactions with aromatic rings in chemical and biological recognition. Angewandte Chemie, International Edition 42:1210–1250.
12. Poppe L (2001) Methylidene-imidazolone: A novel electrophile for substrate activation. Current Opinion in Chemical Biology 5:512–524.
13. Tobias DJ (2001) Electrostatics calculations: Recent methodological advances and applications to membranes. Current Opinion in Structural Biology 11:253–261.
14. Nagy PI (1999) Theoretical calculations for the conformational/tautomeric equilibria of biologically important molecules in solution. Recent Research Developments in Physical Chemistry 3:1–21.
15. He YG, Wu CY, Kong W (2004) Photophysics of methyl-substituted uracils and thymines and their water complexes in the gas phase. Journal of Physical Chemistry A 108:943–949.
16. Andersen LH, Nielsen IB, Kristensen MB, El Ghazaly MOA, Haacke S, Nielsen MB, Petersen MA (2005) Absorption of schiff-base retinal chromophores in vacuo. Journal of the American Chemical Society 127:12347–12350.
17. Levine RD, Bernstein RB (1987) Molecular Reaction Dynamics and Chemical Reactivity. Oxford University Press, New York.
18. Gobbato A, Cestari S, Nilceo M, Cintia G (2005) Ultraviolet A photoprotection: Aging and cutaneous mast cells. Journal of the American Academy of Dermatology 52:96.
19. Mann MB, Swick AR, Gilliam AC, Luo G, McCormick TS (2005) UVB accelerates photo-aging in a Rothmund-Thomson syndrome mouse model. Journal of Investigative Dermatology 124:A76.

20. Ullrich S, Schultz T, Zgierski MZ, Stolow A (2004) Electronic relaxation dynamics in DNA and RNA bases studied by time-resolved photoelectron spectroscopy. Physical Chemistry Chemical Physics 6:2796–2801.
21. Kang H, Lee KT, Jung B, Ko YJ, Kim SK (2002) Intrinsic lifetimes of the excited state of DNA and RNA bases. Journal of the American Chemical Society 124:12958–12959.
22. Pecourt JML, Peon J, Kohler B (2001) DNA excited-state dynamics: Ultrafast internal conversion and vibrational cooling in a series of nucleosides. Journal of the American Chemical Society 123:10370–10378.
23. Gustavsson T, Sharonov A, Onidas D, Markovitsi D (2002) Adenine, deoxyadenosine and deoxyadenosine 5 '-monophosphate studied by femtosecond fluorescence upconversion spectroscopy. Chemical Physics Letters 356:49–54.
24. Pal SK, Peon J, Zewail AH (2002) Ultrafast decay and hydration dynamics of DNA bases and mimics. Chemical Physics Letters 363:57–63.
25. Reuther A, Iglev H, Laenen R, Laubereau A (2000) Femtosecond photo-ionization of nucleic acid bases: Electronic lifetimes and electron yields. Chemical Physics Letters 325:360–368.
26. Crespo-Hernandez CE, Cohen B, Kohler B (2005) Base stacking controls excited-state dynamics in A.T DNA. Nature (London, United Kingdom) 436:1141–1144.
27. Nir E, Muller M, Grace LI, de Vries MS (2002) REMPI spectroscopy of cytosine. Chemical Physics Letters 355:59–64.
28. Nir E, Janzen C, Imhof P, Kleinermanns K, de Vries MS (2001) Guanine tautomerism revealed by UV-UV and IR-UV hole burning spectroscopy. Journal of Chemical Physics 115:4604–4611.
29. Plutzer C, Nir E, de Vries MS, Kleinermanns K (2001) IR-UV double-resonance spectroscopy of the nucleobase adenine. Physical Chemistry Chemical Physics 3:5466–5469.
30. Chin W, Mons M, Dimicoli I, Piuzzi F, Tardivel B, Elhanine M (2002) Tautomer contributions to the near UV spectrum of guanine: Towards a refined picture for the spectroscopy of purine molecules. European Physical Journal D: Atomic, Molecular and Optical Physics 20:347–355.
31. Brady BB, Peteanu LA, Levy DH (1988) The electronic-spectra of the pyrimidine-bases uracil and thymine in a supersonic molecular-beam. Chemical Physics Letters 147:538–543.
32. He YG, Wu CY, Kong W (2003) Decay pathways of thymine and methyl-substituted uracil and thymine in the gas phase. Journal of Physical Chemistry A 107:5145–5148.
33. Hedayatullah M (1981) Alkylation of pyrimidines in phase-transfer catalysis. Journal of Heterocyclic Chemistry 18:339–342.
34. Clark LB, Peschel GG, Tinoco I, Jr (1965) Vapor spectra and heats of vaporization of some purine and pyrimidine bases. Journal of Physical Chemistry 69:3615–3618.
35. Kim SK, Lee W, Herschbach DR (1996) Cluster beam chemistry: Hydration of nucleic acid bases; ionization potentials of hydrated adenine and thymine. Journal of Physical Chemistry 100:7933–7937.
36. Becker RS, Kogan G (1980) Photophysical properties of nucleic acid components. 1. The pyrimidines: Thymine, uracil, N,N-dimethyl derivatives, and thymidine. Photochemistry and Photobiology 31:5–13.
37. Hold U, Lenzer T, Luther K, Reihs K, Symonds AC (2000) Collisional energy transfer probabilities of highly excited molecules from kinetically controlled selective ionization (KCSI). I. The KCSI technique: Experimental approach for the determination of P(E',E) in the quasicontinuous energy range. Journal of Chemical Physics 112:4076–4089.
38. Sobolewski AL, Domcke W, donder-Lardeux C, Jouvet C (2002) Excited-state hydrogen detachment and hydrogen transfer driven by repulsive 1ps* states: A new paradigm for nonradiative decay in aromatic biomolecules. Physical Chemistry Chemical Physics 4:1093–1100.

39. Salet C, Bensasson R (1975) Studies on thymine and uracil triplet excited state in acetonitrile and water. Photochemistry and Photobiology 22:231–235.
40. Honnas PI, Steen HB (1970) X-ray- and uv-induced excitation of adenine, thymine, and the related nucleosides and nucleotides in solution at 77.deg.K. Photochemistry and Photobiology 11:67–76.
41. Goerner H (1990) Phosphorescence of nucleic acids and DNA components at 77 DegK. Journal of Photochemistry and Photobiology B: Biology 5:359–377.
42. Wood PD, Redmond RW (1996) Triplet state interactions between nucleic acid bases in solution at room temperature: Intermolecular energy and electron transfer. Journal of the American Chemical Society 118:4256–4263.
43. Lorentzon J, Fuelscher MP, Roos BO (1995) Theoretical Study of the electronic spectra of uracil and thymine. Journal of the American Chemical Society 117:9265–9273.
44. Baraldi I, Bruni MC, Costi MP, Pecorari P (1990) Theoretical study of electronic spectra and photophysics of uracil derivatives. Photochemistry and Photobiology 52:361–374.
45. Broo A, Pearl G, Zerner MC (1997) Development of a hybrid quantum chemical and molecular mechanics method with application to solvent effects on the electronic spectra of uracil and uracil derivatives. Journal of Physical Chemistry A 101:2478–2488.
46. O'Donnell TJ, Lebreton PR, Petke JD, Shipman LL (1980) Ab initio quantum mechanical characterization of the low-lying cation doublet states of uracil. Interpretation of UV and x-ray photoelectron spectra. Journal of Physical Chemistry 84:1975–1982.
47. Kim NJ, Jeong G, Kim YS, Sung J, Kim SK, Park YD (2000) Resonant two-photon ionization and laser induced fluorescence spectroscopy of jet-cooled adenine. Journal of Chemical Physics 113:10051–10055.
48. Nir E, Kleinermanns K, Grace L, de Vries MS (2001) On the photochemistry of purine nucleobases. Journal of Physical Chemistry A 105:5106–5110.
49. Luhrs DC, Viallon J, Fischer I (2001) Excited state spectroscopy and dynamics of isolated adenine and 9-methyladenine. Physical Chemistry Chemical Physics 3:1827–1831.
50. Broo A (1998) A Theoretical investigation of the physical reason for the very different luminescence properties of the two isomers adenine and 2-Aminopurine. Journal of Physical Chemistry A 102:526–531.
51. Lim EC (1986) Proximity effect in molecular photophysics: Dynamical consequences of pseudo-Jahn-Teller interaction. Journal of Physical Chemistry 90:6770–6777.
52. Ismail N, Blancafort L, Olivucci M, Kohler B, Robb MA (2002) Ultrafast decay of electronically excited singlet cytosine via pi,pi* to n(o)pi* state switch. Journal of the American Chemical Society 124:6818–6819.
53. Wanna J, Menapace JA, Bernstein ER (1986) Hydrogen bonded and non-hydrogen bonded van der Waals clusters: Comparison between clusters of pyrazine, pyrimidine, and benzene with various solvents. Journal of Chemical Physics 85:1795–1805.
54. Brealey GJ, Kasha M (1955) The role of hydrogen bonding in the n -> p* blue-shift phenomenon. Journal of the American Chemical Society 77:4462–4468.
55. Kim NJ, Kang H, Jeong G, Kim YS, Lee KT, Kim SK (2000) Anomalous fragmentation of hydrated clusters of DNA base adenine in UV photoionization. Journal of Physical Chemistry A 104:6552–6557.
56. Kang H, Lee KT, Kim SK (2002) Femtosecond real time dynamics of hydrogen bond dissociation in photoexcited adenine-water clusters. Chemical Physics Letters 359:213–219.
57. Matsika S (2004) Radiationless decay of excited states of uracil through conical intersections. Journal of Physical Chemistry A 108:7584–7590.

58. Hare PM, Crespo-Hernandez CE, Kohler B (2007) Internal conversation to the electronic ground state occurs via two distinct pathways for pyrimidine bases in aqueous solution. Proceedings of the National Academy of Sciences of the United States of America 104:435–440.
59. Hare PM, Crespo-Hernandez CE, Kohler B (2006) Solvent-dependent photophysics of 1-Cyclohexyluracil: ultrafast branching in the initial bright state leads nonradiatively to the electronic ground state and a long-lived 1np state. Journal of Physical Chemistry B 110:18641–18650.
60. Crespo-Hernandez CE, Cohen B, Hare PM, Kohler B (2004) Ultrafast excited-state dynamics in nucleic acids. Chemical Reviews (Washington, DC, United States) 104:1977–2019.
61. Russmann C, Stollhof J, Weiss C, Beigang R, Beato M (1998) Two wavelength femtosecond laser induced DNA-protein crosslinking. Nucleic Acids Research 26:3967–3970.
62. Schreier WJ, Schrader TE, Koller FO, Gilch P, Crespo-Hernandez CE, Swaminathan VN, Carell T, Zinth W, Kohler B (2007) Thymine dimerization in DNA is an ultrafast photoreaction. Science (Washington, DC, United States) 315:625–629.